Estimation techniques for timing mismatch in Time-interleaved Analog-to-Digital Converters: Limitations and solutions

Han Le Duc*, Chadi Jabbour*, Patricia Desgreys*, and Van Tam Nguyen*‡
*Institut Mines-Télécom, Télécom ParisTech, CNRS/LTCI, 46 Rue Barrault, 75013 Paris, France
‡Department of Electrical Engineering, Stanford University, Stanford, CA 94305, USA
Email: han.le-duc@telecom-paristech.fr

***Abstract*—Time interleaving (TI) is one of the best approaches to relax the speed-power trade-off of analog-to-digital converters (ADC). However, channel mismatches especially timing can limit the resolution of TIADC if they are not addressed properly. To achieve an efficient calibration for these errors, the most difficult task is the error estimation in the digital domain. The correction is less problematic and can be done either in digital domain or in the analog domain. Two big families of estimation techniques are commonly employed: the free-band estimation and the cross-correlation estimation. This paper reviews and analyses these estimation techniques and highlights their limitations. It also presents solutions to overcome these limitations.**

I. Introduction

The Time-interleaved analog-to-digital converter (TIADC) is an interesting solution to achieve high speed, high resolution and power-speed tradeoff relaxation [1]. However, the mismatch errors between the individual channels degrade the resolution of TIADCs. In practice, the critical issue in high speed designs is clock skew since its impact increases with the input frequency and overshadows other nonidealities for broadband inputs [1]. Because of this, most of recent research effort in this field has focused on coping with timing mismatches such as in [1]–[3].

The clock skew calibration technique consists of correction and estimation. The correction scheme is either done in digital domain using error subtraction [3] or in analog domain by adjusting a variable-delay line in clock buffers [1]. These correction schemes exhibit good performance and simple way to implement. The most primary challenge for calibration is the estimation in digital domain, especially input frequency dependent error parameters such as clock skews. Timing mismatch estimation can be performed either online or offline. In offline estimation approach [4] of timing mismatch, a special operation phase dedicated for estimation is required. During this phase, a pilot signal is injected into the ADC and results thereby in an interruption in its operation. Therefore, these techniques are not well suited for communication applications because their operation does not allow long interruptions and also due to strong variation of the circuit parameters with the changes of the operation environment. In this case, online estimation schemes are preferred because they enable the ADCs to operate in nominal mode while clock skews are estimated [2], [3], [5]–[7]. There are two main families of online estimation techniques including cross-correlation estimation [2], [3] and free band estimation [6], [7]. These techniques show good performance and do not require a very complex circuit implementation. However, they suffer from some limitations which can lead to a divergence in the parameter estimations. Unfortunately, most of the papers in the literature do not discuss and study these limitations. In this paper, we analyze and highlight the limitations of two classical families of estimation mechanisms: cross-correlation and free band (mismatch band) estimation. Solutions for these limitations are then proposed and analyzed by the means of analytical calculation and simulation.

The rest of the paper is organized as follows. Section II analyses the limitations of the cross-correlation estimation schemes and propose solutions to overcome these simulation. Section III is dedicated to highlight the limitations of the mismatch band estimation algorithms and propose solutions for these limitations. Conclusions are finally drawn in Section IV.

II. Cross-correlation based techniques

A. Limitation Analysis

Cross-correlation based estimation approaches [1]–[3] require the input signal to be wide-sense stationary (WSS). In these approaches, the clock skews are estimated based on either the pairwise cross-correlation of sub-ADC outputs [1] or the cross-correlation between compensated signals and aliasing signals due to timing skews [2], [3]. In [1], the author used the cross-correlation to measure the clock skews as illustrated in Fig. 1. The operation of the estimation

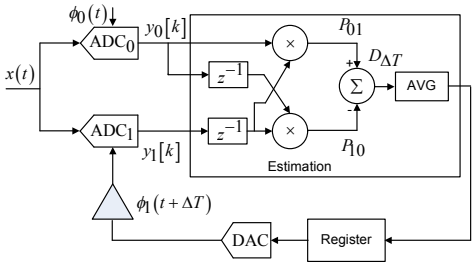

Fig. 1: Cross-correlation estimation algorithm [1].

algorithm is as follows. Let assume that there are no gain and offset mismatches and that τ_m, $\delta t_m = \frac{\tau_m}{T}$ are deterministic relative and absolute timing deviation of the m^{th} channel ADC, respectively where T is the sampling period of TIADCs. Averaging (AVG) the cross-product (or computing the cross-correlations) P_{01}, P_{10} between sub-ADC delayed or without delayed samples produces the DC values. The difference of P_{01}, P_{10} is the DC value linearly proportional to timing mismatch $\Delta_T = \delta t_1 - \delta t_0$ between sub-ADC channels as [1].

$$P_{01} - P_{10} = y_1[k-1]\, y_0[k] - y_1[k-1]\, y_0[k-1] \propto \Delta T. \quad (1)$$

To analyze the limitations of this technique, let us consider the input signal containing two frequency components ω_a, ω_b as

$$x(t) = A_a \cos\left(\frac{\omega_a}{T}t + \phi_a\right) + A_b \cos\left(\frac{\omega_b}{T}t + \phi_b\right). \quad (2)$$

Ignoring quantization effects, the digital output sequence $y_m[k]$ of the m^{th} channel ADC is expressed by

$$y_m[k] = y_m(kT_s) = x\left(kMT_s + mT_s + \tau_m\right). \quad (3)$$

From (2), (3) and Fig. 1, the cross-correlation is expressed by

$$\begin{aligned} P_{01} \quad = \quad & \tfrac{A_a^2}{2}\cos\left(-\omega_a + \tfrac{\omega_a}{T}\Delta T\right) \\ & + \tfrac{A_b^2}{2}\cos\left(-\omega_b + \tfrac{\omega_b}{T}\Delta T\right) + res[k] \end{aligned} \quad (4)$$

where

$$res\,[k] = \frac{A_a^2}{2}\cos\left[2\omega_a Mk+\phi_{c1}\right]+\frac{A_b^2}{2}\cos\left[2\omega_b Mk+\phi_{c2}\right] + \frac{A_aA_b}{2}\left\{\cos\left[\left(\omega_a+\omega_b\right)Mk+\phi_{c3}\right] + \cos\left[\left(\omega_a-\omega_b\right)Mk+\phi_{c4}\right]\right\} + \frac{A_bA_a}{2}\left\{\cos\left[\left(\omega_b+\omega_a\right)Mk+\phi_{c5}\right] + \cos\left[\left(\omega_a-\omega_b\right)Mk+\phi_{c6}\right]\right\}. \quad (5)$$

ϕ_{ci} are constant phase and are independent of k. The first and second term of (4) are independent of k and they are measures for timing mismatch estimation. The $res[k]$ term in general is filtered by AVG filter. Careful analysis with $\omega = 2\pi\frac{f}{f_s}$, if

$$f_a \text{ or } f_b = k\frac{f_s}{2M} \quad (6a)$$

$$\text{or } f_a \pm f_b = k\frac{f_s}{M} \quad (6b)$$

where k is integer, $res[k]$ is then independent of k too. Thus, it is non-zero DC components after AVG filter, hence (1) may be incomplete or the estimation is inaccurate.

In general, the expression (6) presents the limitations (or input signal restriction) of the cross-correlation estimation algorithms. It means that if the input signal contains two frequency components f_a, f_b fulfilling the expression (6), the input and the unwanted images due to time-interleaving are overlapped [8]. As a result, estimator does not distinguish the signal from the undesired tones.

B. Solutions for the limitations of cross-correlation estimation techniques

1) Solutions for the limitation (6a): In the case of the input signal only satisfying expression (6a), there is divergence on the parameter estimation as interpretated in Section II-A. To overcome this limitation, notch filters are cascaded in front of the AVG filter to attenuate the amplitudes of these input frequency components. This solution prevails upon zero values of $res[k]$, timing mismatch is properly estimated based on (1).

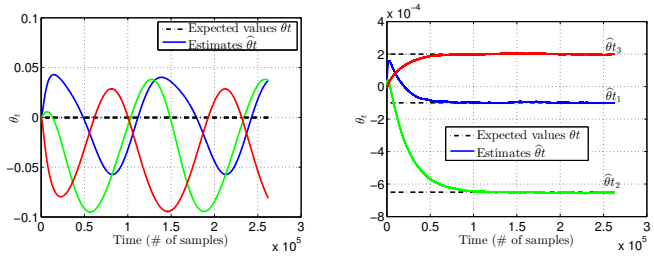

(a) (b)

Fig. 2: Convergence behavior: (a) without notch filters and (b) with notch filters.

To evaluate and analyse the limitation (6a) as well as the proposed solution for this limitation, the all-digital calibration proposed in [3] and a 4-channel 11bit TIADC with sampling rate of 2.7GHz are used for simulation. Timing skews are Gaussian distribution numbers with zero mean and standard deviation of 0.33ps. The input contains seven sinusoid tones at the frequencies $[0.125,\ 0.25,\ 0.375,\ 0.05,\ 0.18,\ 0.29,\ 0.405]\times f_s$, i.e. it has special tones at frequencies $k\frac{f_s}{8}, k = \{1,2,3\}$. Three digital notch filters whose magnitude responses are shown in Fig. 3(a), are cascaded before the AVG filter. Fig. 2 shows the convergence behavior with and without using the notch filters. As can be seen, the clock skew estimates converge to their expected values for the case using notch filters in contrast to the case without notch filters. After calibration, images are then reduced to noise floor as shown in Fig. 3(b).

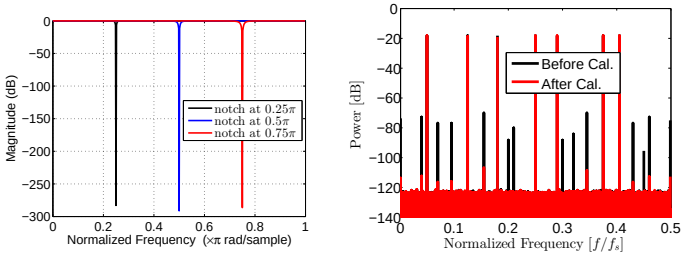

(a) (b)

Fig. 3: (a) Magnitude responses of cascaded notch filters and (b) output spectrum before/after calibration with the notch filters.

2) Solutions for the limitation (6b): To cope with this limitation, it is necessary to separate the input and aliasing signals. Let assume the input $x(t)$ to be bandlimted to f_c as shown in Fig. 4. If f_c is less than the bandwidth $\frac{f_s}{2M}$ of the sub-ADCs, there is no overlap between the spurious and input signals. The algorithm can be used to accurately estimate the unknown timing skew coefficients. If $\frac{f_s}{2M} < f_c < f_s$, for 2-channel time-interleaved ADCs, a proposed solution is to use a band-stop filter in front of the AVG filter in the estimation part. Let us denote the frequency response of the band-stop filter by

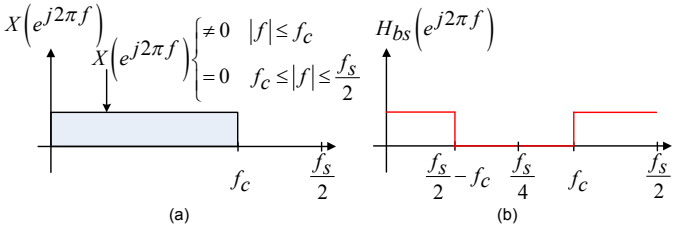

Fig. 4: (a) Bandlimited input spectra and (b) Frequency response of the band-stop filter

$H_{bs}\left(e^{j2\pi f}\right)$ shown in Fig. 4(b), the band-stop filter removes the frequency band $\frac{f_s}{2} - f_c \le |f| \le f_c$ where input and images are overlapped. This separates the input spectra part in the band $\left(0, \frac{f_s}{2} - f_c\right]$ from the spurious spectra part in the band $\left[f_c, \frac{f_s}{2}\right)$ due to the timing skews. Distinguishing the input from spurs makes estimation working properly and accurately.

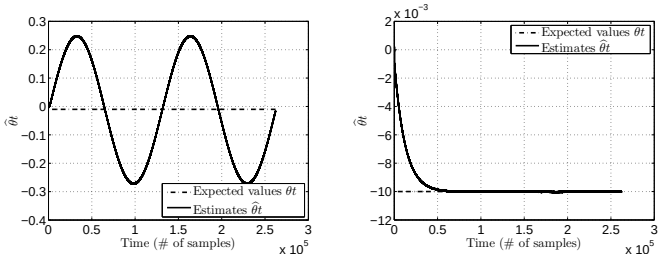

(a) (b)

Fig. 5: Convergence behavior of the timing mismatch coefficients: (a) with and (b) without band-stop filters.

To verify the efficiency of the proposed solution, a two-channel 11-bit TIADC clocked at 2.7GHz and a simulated input at frequencies $f_{in} = [0.05\ 0.15\ 0.35\ 0.4] \times f_s$ are simulated for this analysis. The clock skew values are $[0,\ 0.02] \times T_s$. The digital band-stop filter has low and high cutoff frequencies of $0.1f_s$ and $0.4f_s$, respectively. Its frequency response is shown in Fig. 6(a). The clock skew coefficient

estimates diverge without using the digital band-stop filter as shown in Fig. 5(a) in contrast to the convergence behavior in Fig. 5(b) where the band-stop filter is used. The output spectrum before and after calibration using the band-stop filter is shown in Fig. 6(a) where spurs due to timing skew are reduced from -40dBFS to -95dBFS.

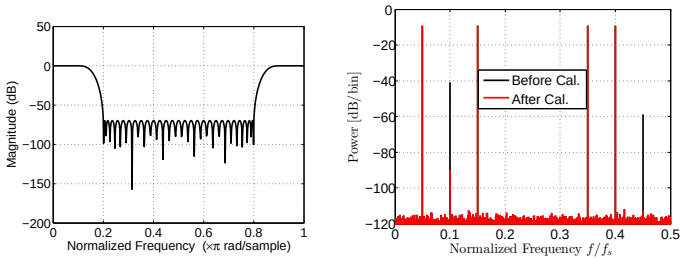

(a) (b)

Fig. 6: (a) Magnitude response of the band-stop filter and (b) Output spectrum before and after calibration using the band-stop filter.

Note that for a number of channels larger than two, this solution can not be applied. This is due to the fact that it is impossible to separate the non-overlapped frequency bands of images and input for wideband bandlimited input signals. In practice, the presence of each signal in the wanted bandwidth has its own probability and the two signals are rarely present at the same time for a long time, i.e. the sum (or the difference) of two frequency components is not exactly equal $k\frac{f_s}{2M}$. Actually, the frequency deviation $\Delta f \times f_s$ of two arbitrary frequency components in real input spectrum is not zero. Let us study the impact of Δf on the efficiency of the cross-correlation estimation schemes. Assume that $f_a \pm f_b = k\frac{f_s}{M} + \Delta f \times f_s$ where $\Delta f \neq 0$

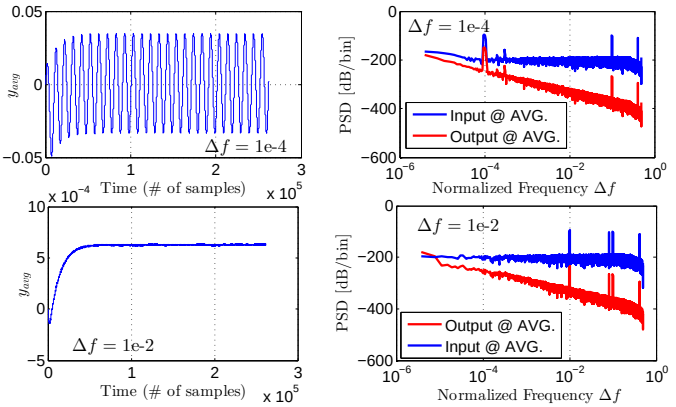

Fig. 7: Left side: Convergence speed of one clock skew coefficient and right side: Signal spectrum at input/output AVG filter.

and it is so-called frequency deviation factor. The 4-channel 11-bit TIADC is used for this analysis. The left and right sides of Fig. 7 show the timing skew estimate convergence speed and the spectrum of input/output signals of AVG filter. As can be seen, with small $\Delta f = 10^{-4}$, the frequency component $\Delta f \times f_s$ is inside the bandwidth of the AVG filter i.e., it is not filtered as shown in the right side top of Fig. 7. In other words, the $res[k]$ term in (4) is not zero. Thus, there is a big variation on the clock skew estimates as illustrated in the top-left corner of Fig. 7. In contrast, with higher $\Delta f = 10^{-2}$, the frequency component $\Delta f \times f_s$ is almost completely filtered by averaging filter as shown in the bottom-right corner of Fig. 7, leading that the clock skew coefficients converge to their expected values as drawn in the bottom-left corner of Fig. 7. Fig. 8 shows the SNDR/SFDR versus various Δf after calibration using the Monte-Carlo simulation. At the deviation factor $\Delta f = 0.01$, the SNDR after calibration is 67dB which is equal to its value in the no-mismatch case. As above demonstrated, the

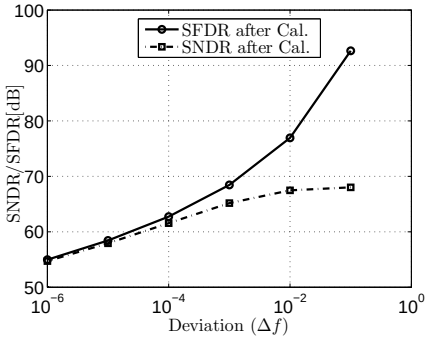

Fig. 8: Minimum SNDR/SFDR versus Δf after calibration using the Monte-Carlo simulation.

large fluctuations occur on the parameter estimates with smaller Δf and $\Delta f \neq 0$. To mitigate these fluctuations, smaller step size μ is chosen, however the cost is slow convergence speed. In other words, the smaller Δf, the longer convergence speed.

III. Free-band Based Estimation Techniques

In free-band based estimations [6], [7], the bandlimited input signal is assumed to be slightly oversampled, generating a frequency band that contains only spurs due to the clock skews without the input. This frequency band is called *free-band* or *mismatch band*. The clock skew estimates are determined by using a LMS algorithm to minimize the errors due to the timing mismatch in the free band. Vogel *et al.* [6] proposed an adaptive estimation technique of timing skews illustrated in Fig. 9. The error signal $e[n]$ due to timing mismatch is

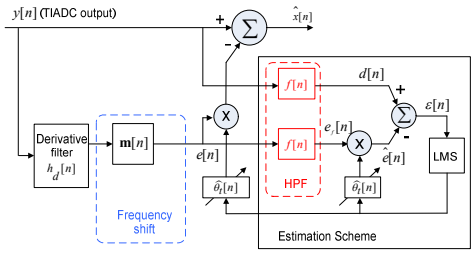

Fig. 9: All-digital calibration of timing skew proposed by Vogel et al. in [6].

reconstructed by a derivative filter with the impulse response $h_d[n]$ and a modulation vector $\mathbf{m}[n]$ in Eq.13 [6]. To estimate the timing skew coefficients, High-Pass Filters (HPFs) $f[n]$ are designed to filter out signal errors and attenuate the input signal energy in the mismatch band. As can be seen from Fig. 9, the error signal $d[n]$ is the reference signal in the LMS algorithm, which enables the sample-time error estimation. Applying LMS to error function $\varepsilon[n] = d[n] - \hat{e}[n]$ yields the updated equation as [6]

$$\hat{\theta}t\,[n+1] = \hat{\theta}t\,[n] + \mu\varepsilon\,[n]\,e_f\,[n]\,, \tag{7}$$

where μ is the step size of LMS. Obviously, the timing mismatch coefficients is updated an amount being cross-product of two error signals (clock skew induced error signal and its estimate) as expressed in (7), hence relaxing the requirements of the input statistical properties.

A. Advantages of free-band based estimation techniques

In general, the free frequency band approach does not suffer from the limitations presented in (6) of the cross-correlation based calibration since the free-band based calibration techniques constrain the shape of input spectrum and relax the requirements of the input statistical properties.

The estimation technique proposed by Vogel *et al.* [6] and a 4-channel 11-bit TIADC clocked at 2.7GHz are used for simulation. Timing skews are Gaussian distribution numbers with zero mean and standard deviation of 0.33ps. The step size is $\mu = 2^{-10}$.

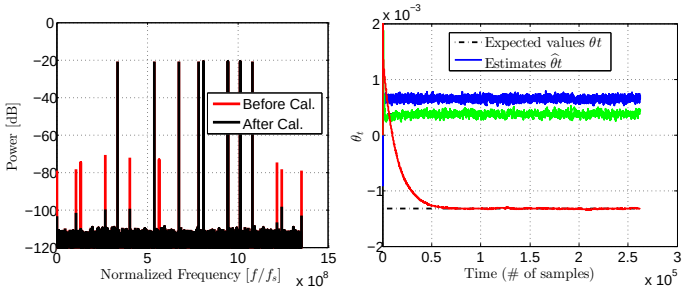

(a) (b)

Fig. 10: Output spectrum (a) before and (b) after calibration for input belonging the limitations of cross-correlation estimation.

To demonstrate that the free-band estimation does not suffer from the limitation expressed in (6), a simulation is tested for the input signal contains frequency components at $f_{in} = [0.125,\ 0.2,\ 0.3,\ 0.375,\ 0.29,\ 0.35,\ 0.25,\ 0.4] \times f_s$ satisfying (6). Fig. 10(a) shows the convergence behavior where clock skews converge to their expected values. Moreover, spurs due to timing skews reduce from -75dB to -100dB as shown in Fig. 10(b). As expected, the mismatch band estimation does not suffer from the two limitations of cross-correlation estimation.

B. Limitations of free-band based estimation techniques

The mismatch band estimations in general require that all image's spectra due to timing mismatch must be inside the mismatch band in order to make an accurate estimation. In practice, if the input signal is wideband and occupies most of the ADC bandwidth, this condition is satisfied. Another limitation is its sensitivity to the distortions caused by the nonlinearity of the TIADCs. Actually, non-linearity causes spectrum spreading and thus creates non-linear components in the free frequency band which can lead to a divergence in the estimation algorithm.

Let us now study the impact of non-linearity on the free-band estimation algorithm. For this study, a simple polynomial block is inserted before the ADC to model the non-linear behavior of the ADC: $P(x) = x - 0.05x^3$. The input signal consists of four sinusoid tones at frequencies $[0.05, 0.18, 0.29, 0.405] \times f_s$. Due to non linearity, several inter-modulation products will arise in the free frequency band. If the power of these components is high enough, they can cause the divergence of some the timing mismatch coefficient estimates as can be seen in Fig. 11(a). As a consequence, the spurious images after calibration are not removed as shown in Fig. 11(b). In order to address this problem, the free frequency band clock skew algorithm can be combined with a post-distortion algorithm that also uses the free frequency band approach for estimation [9]. This would allow a mitigation of both the clock skew and the non-linearities of the ADC.

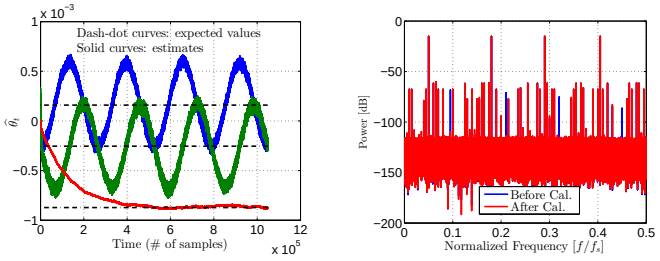

(a) (b)

Fig. 11: (a) Convergence speed and (b) Output spectrum before/after calibration for input suffering from nonlinear distortion model.

IV. Conclusion

This paper has studied and analyzed the limitations of the two main approaches for clock skew estimation in TI ADC. It has also proposed solutions to overcome these limitations. The first main family of estimation is cross-correlation based technique. This technique shows a divergence of the clock skew estimates when the input signal contains two frequency components such that clock skew induced spurious images overlap with the input signal itself. To address this problem, notch filters can be used to remove the components at $k\frac{f_s}{M}$. For two-channel TIADCs, a band-stop filter can be employed to isolate the frequency mismatch bands. The second approach for estimation is the free band technique. This technique relaxes the requirements on the input signal statistical properties. Thus, it does not suffer from the aforementioned limitations of cross-correlation techniques. However, this technique is sensitive to the non-linear distortions of ADC. Actually, non-linearity creates undesired non-linear frequency components in free frequency band with could lead to a divergence in the estimation algorithm. To overcome this limitation, a combined mitigation algorithm for both timing skew and non-linearites should be employed at the TIADC output.

References

[1] B. Razavi, "Design Considerations for Interleaved ADCs," *Solid-State Circuits, IEEE Journal of*, vol. 48, no. 8, pp. 1806–1817, 2013.

[2] J. Matsuno *et al.*, "All-Digital Background Calibration Technique for Time-Interleaved ADC Using Pseudo Aliasing Signal," *Circuits and Systems I: Regular Papers, IEEE Transactions on*, vol. 60, no. 5, pp. 1113–1121, 2013.

[3] H. Le Duc *et al.*, "All-Digital Calibration of Timing Skews for TIADCs Using the Polyphase Decomposition," *IEEE Transactions on Circuits and Systems II: Express Briefs*, vol. 63, no. 1, pp. 99–103, Jan 2016.

[4] L. Kull *et al.*, "A 90GS/s 8b 667mW 64-interleaved SAR ADC in 32nm digital SOI CMOS," in *2014 IEEE International Solid-State Circuits Conference Digest of Technical Papers (ISSCC)*, Feb 2014, pp. 378–379.

[5] K. M. Tsui and S. C. Chan, "A Novel Iterative Structure for Online Calibration of M -channel Time-Interleaved ADCs," *IEEE Transactions on Instrumentation and Measurement*, vol. 63, no. 2, pp. 312–325, Feb 2014.

[6] C. Vogel *et al.*, "Adaptive blind compensation of gain and timing mismatches in M-channel time-interleaved ADCs," in *Electronics, Circuits and Systems, 2008. ICECS 2008. 15th IEEE International Conference on*, 2008, pp. 49–52.

[7] V. Divi and G. W. Wornell, "Blind Calibration of Timing Skew in Time-Interleaved Analog-to-Digital Converters," *Selected Topics in Signal Processing, IEEE Journal of*, vol. 3, no. 3, pp. 509–522, 2009.

[8] M. El-Chammas and B. Murmann, "General Analysis on the Impact of Phase-Skew in Time-Interleaved ADCs," *Circuits and Systems I: Regular Papers, IEEE Transactions on*, vol. 56, no. 5, pp. 902–910, May 2009.

[9] M. Grimm *et al.*, "Joint mitigation of nonlinear rf and baseband distortions in wideband direct-conversion receivers," *IEEE Transactions on Microwave Theory and Techniques*, vol. 62, no. 1, pp. 166–182, Jan 2014.